# Supplementary Materials

Urbanization and the Network Role of Loneliness in Adolescent Suicide Risk: A Four-Stage Analysis Across 87 Countries

## Supplementary Materials

### Urbanization and the Network Role of Loneliness in Adolescent Suicide Risk: A Four-Stage Analysis Across 87 Countries

---

### Table S0. STROBE Checklist

*[To be completed: insert filled STROBE checklist for cross-sectional studies — see von Elm et al. (2007), Lancet 370:1453–1457]*

---

### Figure S0. Participant Flow Diagram

*[To be created: flow diagram showing derivation of Stage 1 complete cases (N = 292,280), Stage 2–3 analytic countries (N = 42, ≥ 2,000 per country), and Stage 4 countries (N = 38, ≥ 500 per country) from total sample of 439,026 across 87 countries and 158 GSHS datasets]*

---

### Supplemental Tables

**Table S1.** Summary of sample sizes, urbanization rates, and macro-level indicators for 42 countries.

*Full data available in processed_data/15_country_summary_v2.csv*

---

**Table S2.** Complete centrality indices (Strength, Expected Influence, Betweenness, Closeness) for all 15 nodes in the global network.

*Full data available in processed_data/01_centrality_global_with_EI.csv*

---

**Table S3.** Centrality comparison across five regional subnetworks.

*Full data available in results/tables/03_regional_centrality.csv*

---

**Table S4.** Complete NCT results for 10 regional pairwise comparisons (1,000 permutations).

*Full data available in results/tables/04_nct_summary_1000perm.csv*

---

**Table S5.** Complete 5 × 5 transfer matrix (AUC + degradation percentages) and XGBoost hyperparameter configuration.

*AUC matrix available in results/tables/06_transfer_auc_matrix.csv; F1-score matrix available in results/tables/07_transfer_f1_matrix.csv*

---

**Table S6.** Cross-regional SHAP coefficients of variation for 12 variables.

*Full data available in results/tables/10_regional_shap_divergence.csv*

---

**Table S7.** Complete results of 132 macro-micro Spearman correlations.

*Full data available in processed_data/13_macro_micro_correlations_v2.csv*

---

**Table S8.** Complete GLMM fixed effects and random effects.

*Fixed effects available in processed_data/25_glmm_fixed_effects.csv; Random effects available in processed_data/25_glmm_random_effects.csv; Random slopes available in processed_data/25_glmm_random_slopes.csv*

---

**Table S9.** Complete SCA results for 432 specifications.

*Full data available in processed_data/26_sca_results.csv*

---

**Table S10.** Complete urbanization moderation results for all 105 edges.

*Full data available in processed_data/35_edge_urbanization_moderation.csv*

---

**Table S11.** Gender-stratified SHAP × urbanization analysis.

*Full data available in processed_data/34_gender_urbanization_correlations.csv*

---

## Supplemental Figures

**Figure S1.** Five WHO regional subnetwork plots (Africa, Americas, Eastern Mediterranean, South-East Asia, Western Pacific). Nodes represent the 15 psychological/behavioral variables; edges represent EBIC-glasso partial correlations. Node size proportional to Strength centrality. Positive edges shown in green, negative edges in red.

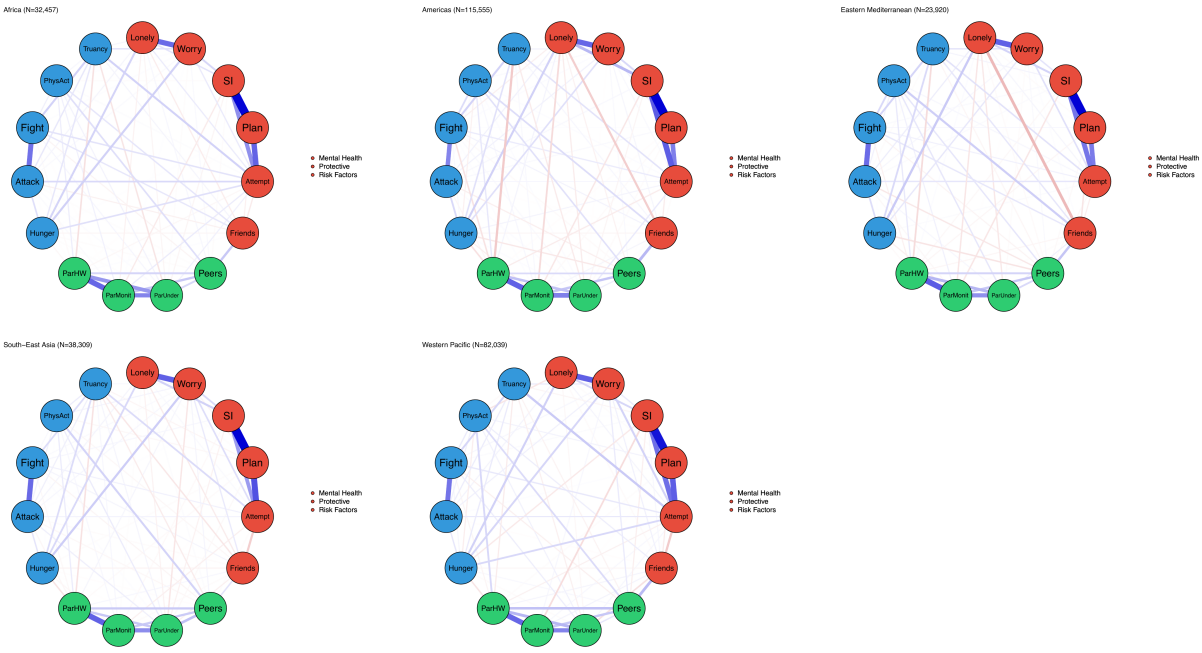


Figure 1: Five WHO Regional Subnetworks

---

**Figure S2.** Bootstrap stability analysis (CS-coefficient = 0.75). Upper panel: case-dropping subset bootstrap for centrality stability; lower panel: edge weight accuracy intervals (1,000 bootstraps). CS-coefficient of 0.75 exceeds the recommended threshold of 0.50, indicating reliable centrality rankings.

---

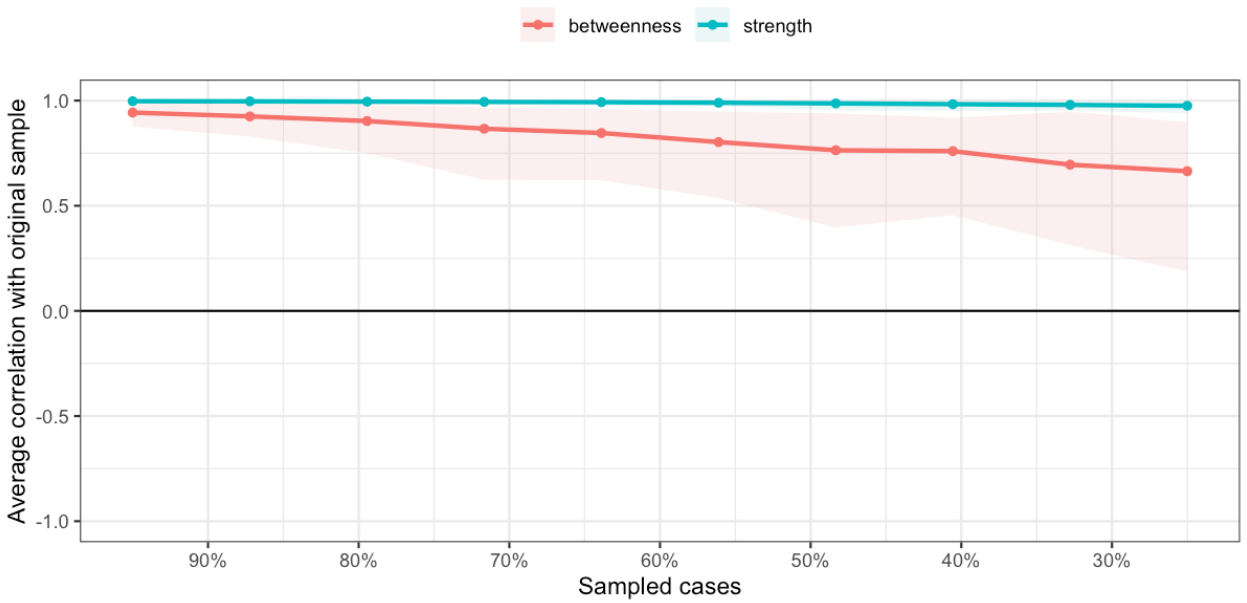


Figure 2: Bootstrap Stability Analysis

**Figure S3.** Regional SHAP importance comparison across five WHO regions. Heatmap of mean absolute SHAP values for 12 predictor variables (rows) across five regions (columns), normalized within each region. Loneliness shows high importance across all regions; physical activity and hunger show larger cross-regional variation.

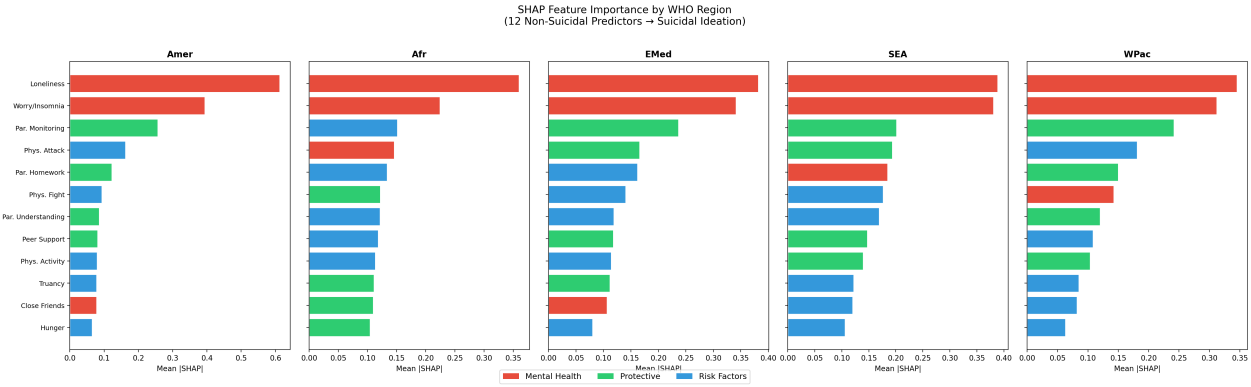


Figure 3: Regional SHAP Importance Comparison

---

**Figure S4.** Cultural sensitivity index for 12 variables across regions. Coefficient of variation (CV) of SHAP importance across the five regional models, indicating which predictors are most culturally variable in their association with suicidal ideation.

---

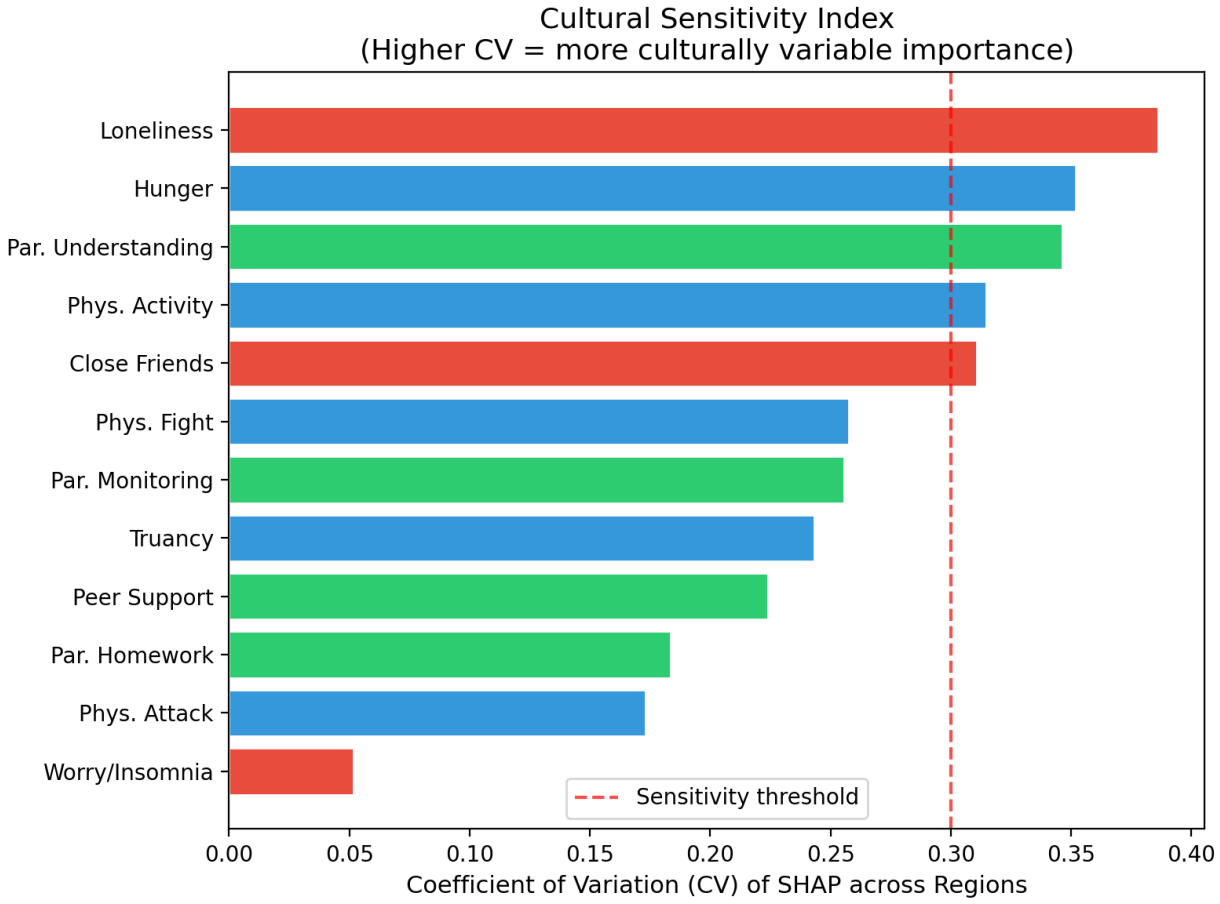


Figure 4: Cultural Sensitivity Index

**Figure S5.** Heatmap of 132 macro-micro associations. Spearman correlations between 11 macro-level indicators (columns) and 12 SHAP importance profiles (rows) across 42 countries. Cells with FDR-corrected $p < .05$ are marked with an asterisk. Urbanization rate shows the strongest and most consistent pattern of association.

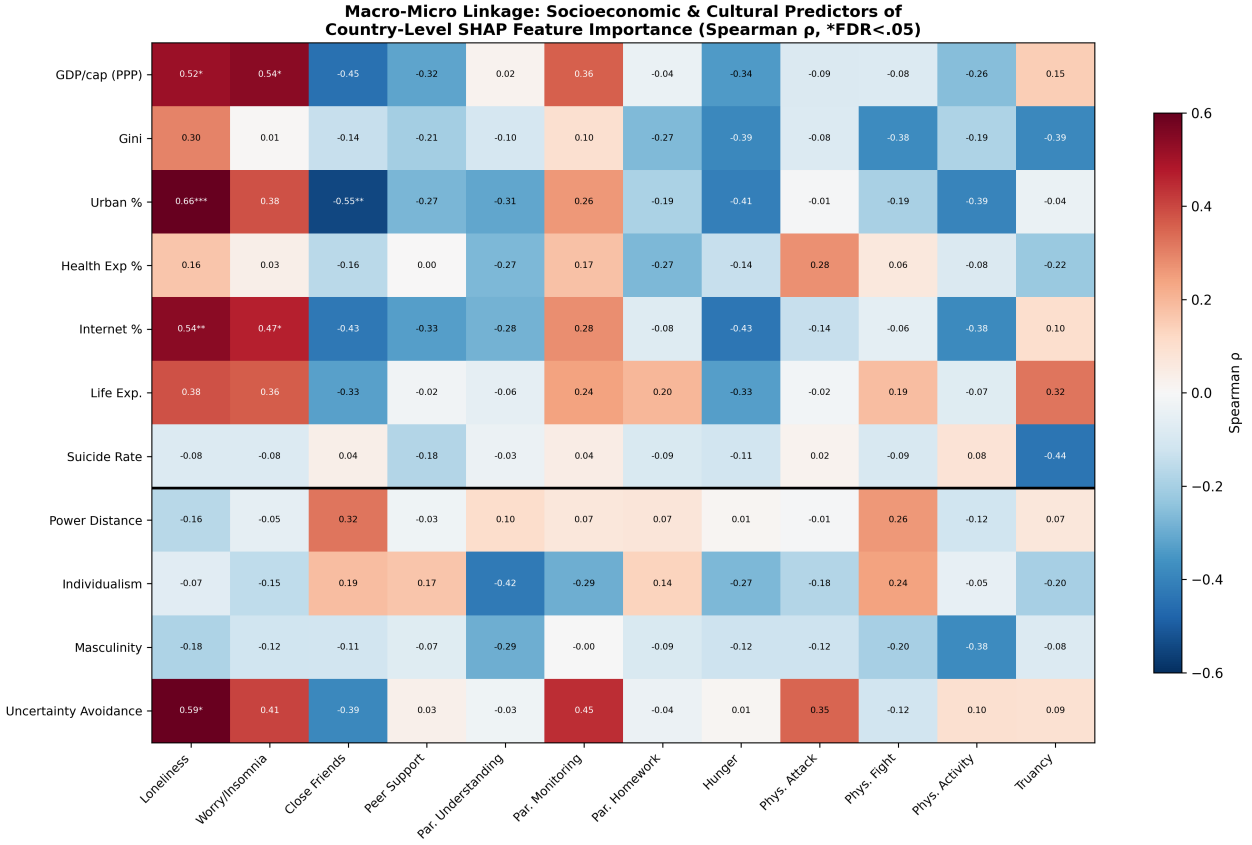


Figure 5: Macro-Micro Association Heatmap

---

**Figure S6.** GLMM fixed effects forest plot. Odds ratios (95% CI) from the individual-level GLMM predicting suicidal ideation (N = 296,863; 42 countries). The loneliness × urbanization interaction term (OR = 1.096, 95% CI [1.053, 1.140], p = 6.2 × 10^−6) is highlighted.

---

**Figure S7.** GLMM random slopes for 42 countries. Country-specific random slopes for the loneliness effect on suicidal ideation, sorted by national urbanization rate. Higher-urbanization countries (right) show systematically stronger loneliness–suicidal ideation associations.

---

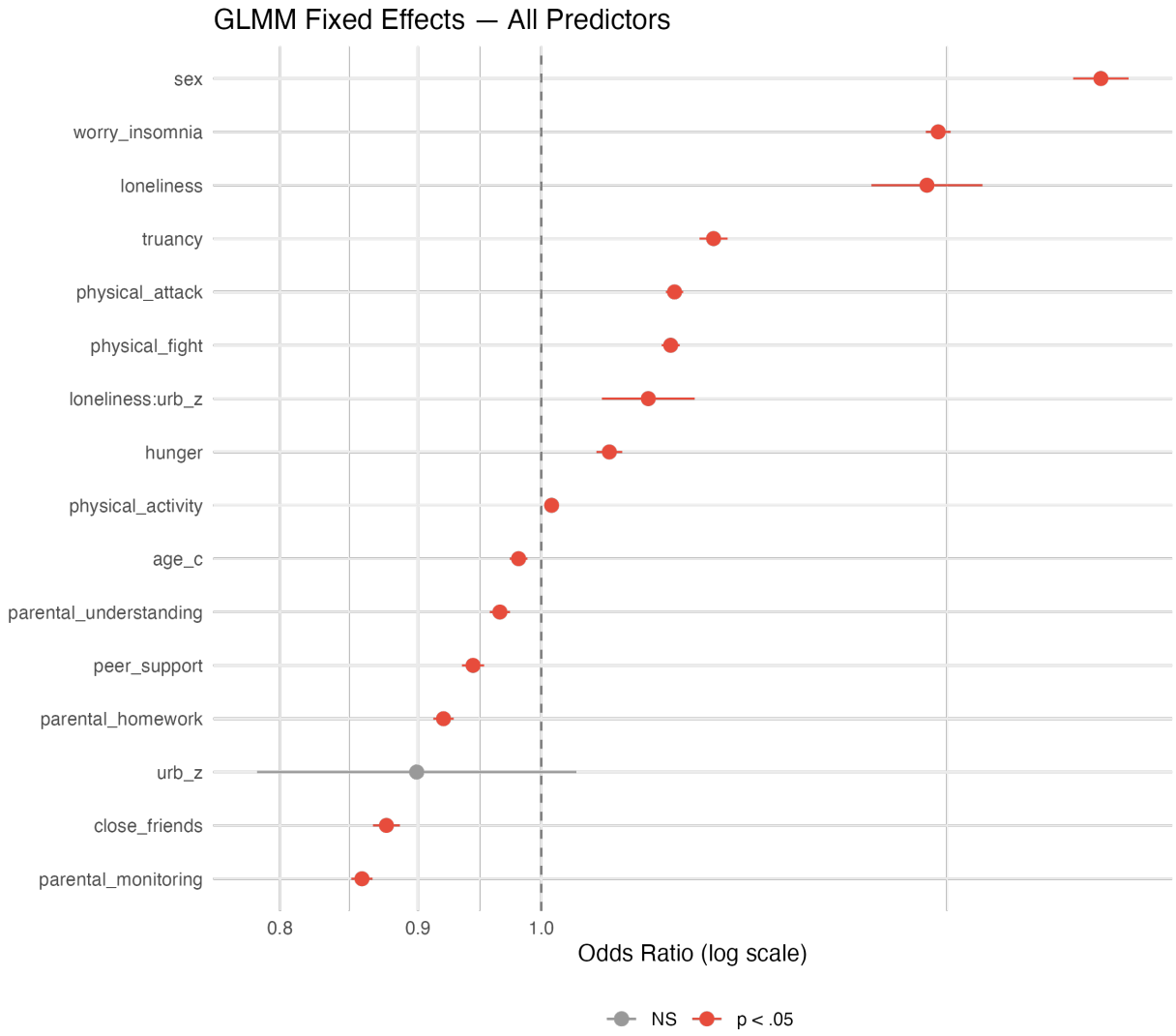


Figure 6: GLMM Fixed Effects Forest Plot

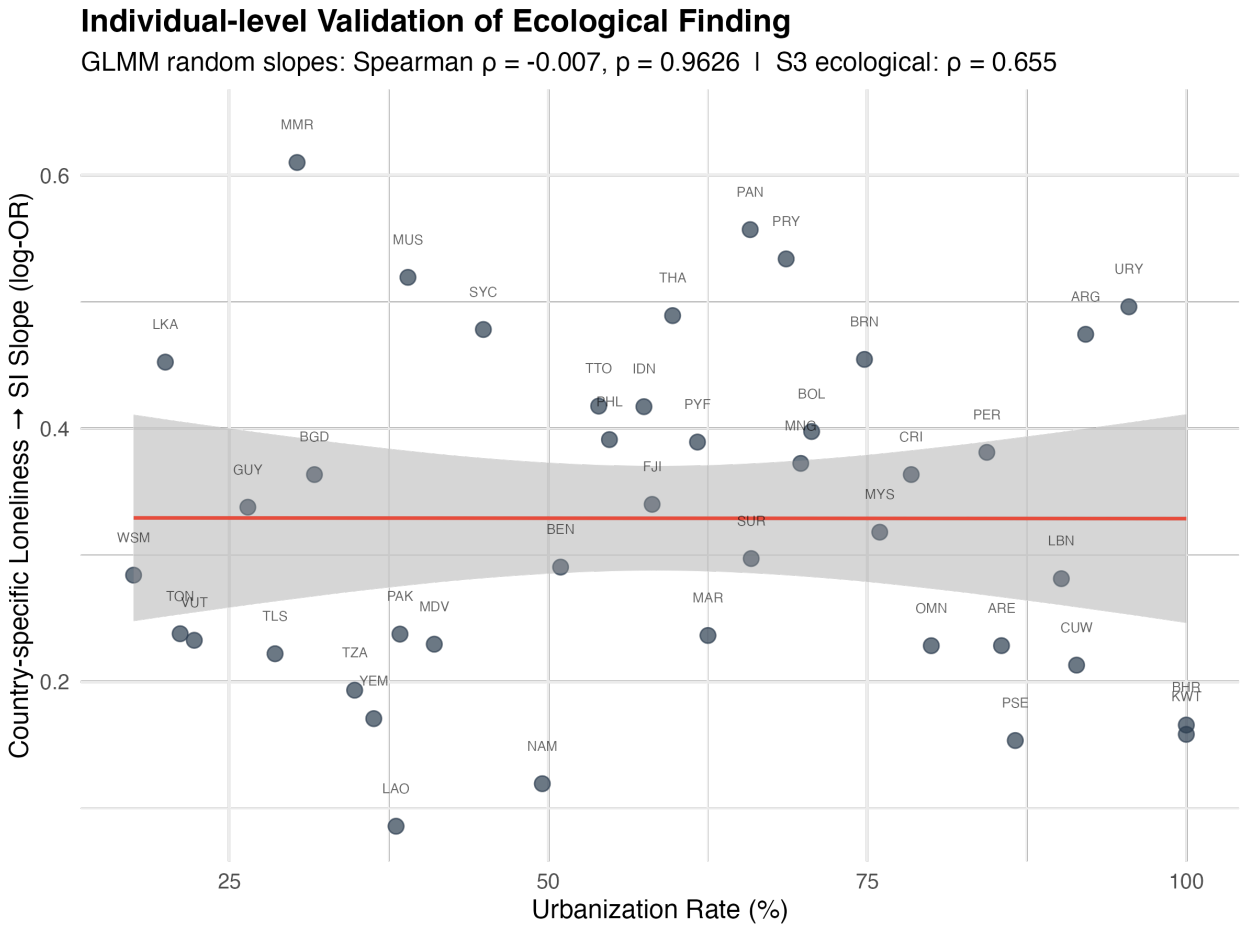


Figure 7: GLMM Random Slopes

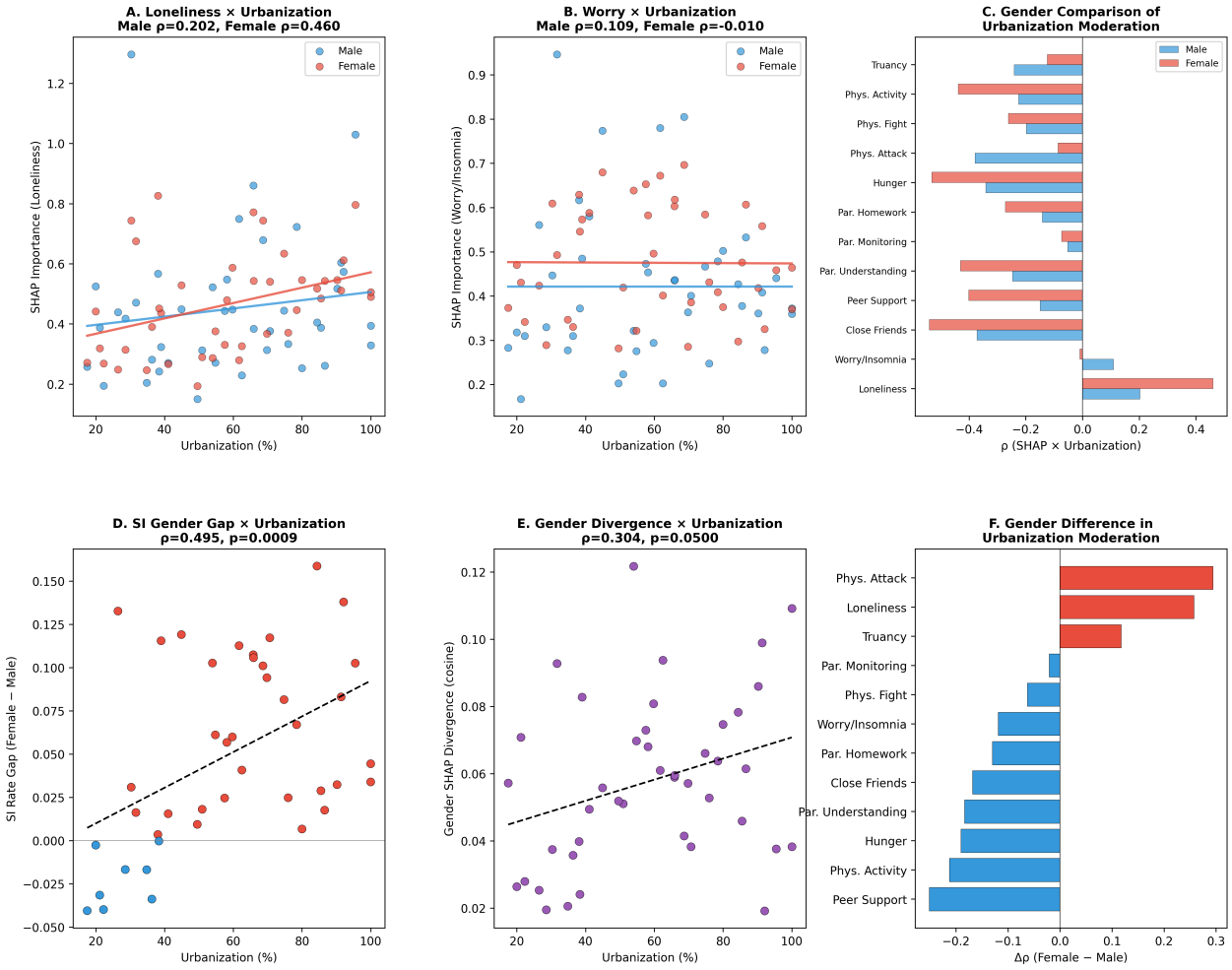


Figure 8: Gender × Urbanization Analysis

**Figure S8.** Gender × urbanization SHAP stratification analysis. Left panel: urbanization–loneliness SHAP correlation by gender (females: r_s = .460, p = .002; males: r_s = .202, p = .199). Right panel: gender gap in suicidal ideation prevalence (female minus male rate) vs. urbanization rate (r_s = .495, p = .0009).

---

**Figure S9.** Ising computational illustration (three panels). **(A)** Node activation probability as a function of urbanization level (comparative statics via exact enumeration of 2^14 = 16,384 states): loneliness and worry-insomnia increase, hunger and physical activity decrease. **(B)** Sigmoid inflection point analysis: loneliness-to-suicidal-ideation intervention effect as a function of urbanization rate, with inflection point at approximately 40.2% urbanization (sensitivity range 22–49% across alpha = 0.5–2.0). **(C)** NIRA intervention heatmap: single-node deactivation effects on suicidal ideation across urbanization gradient; optimal intervention targets shift from worry/hunger (low urbanization) to loneliness (high urbanization). This analysis represents comparative statics on cross-sectional parameters and does not support causal or temporal inference.

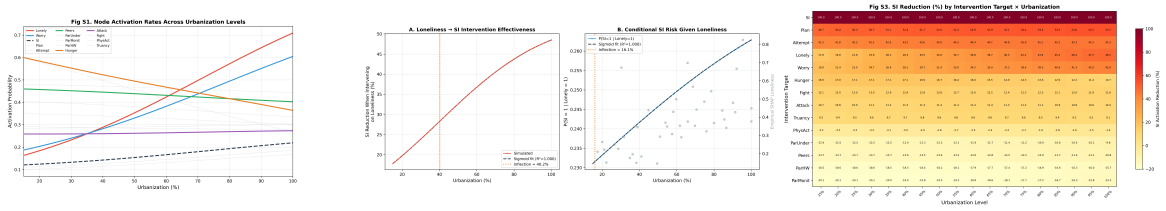


Figure 9: Ising Computational Illustration

---

**Figure S10.** Specification Curve Analysis (432 specifications). Upper panel: interaction coefficients sorted by effect size (orange = p < .05, gray = nonsignificant); 94.4% significant, 100% positive. Lower panel: analytic choices for each specification (outcome, features, covariates, estimator, country threshold). Stratified by outcome: 100% of suicidal ideation and suicide plan specifications significant; 83.3% of suicide attempt specifications significant.

---

**Figure S11.** Robustness checks. **(a)** Partial Spearman correlations (with 95% CI) after controlling for GDP and/or internet penetration; all 17 FDR-significant edges remain significant. **(b)** SHAP stability across five random seeds (mean profile r_s = .919). **(c)** Leave-one-out analysis (N = 42; all iterations significant). **(d)** Overall missingness rate vs. urbanization (r_s = −.454, p = .003), indicating that higher-urbanization countries do not contribute systematically lower-quality data.

---

**Figure S12.** Network rewiring by urbanization. Each of the 105 edges in the 15-node network is colored by the direction and FDR significance of its Spearman correlation with national urbanization rate: red = strengthened in higher-urbanization countries (FDR significant, r_s > 0; n = 5 edges); blue = weakened (FDR significant, r_s < 0; n = 12 edges); gray = non-significant (n = 88 edges). Line width proportional to |r_s|. The pattern reflects a structural shift in which loneliness becomes more central and buffering pathways weaken in higher-urbanization contexts.

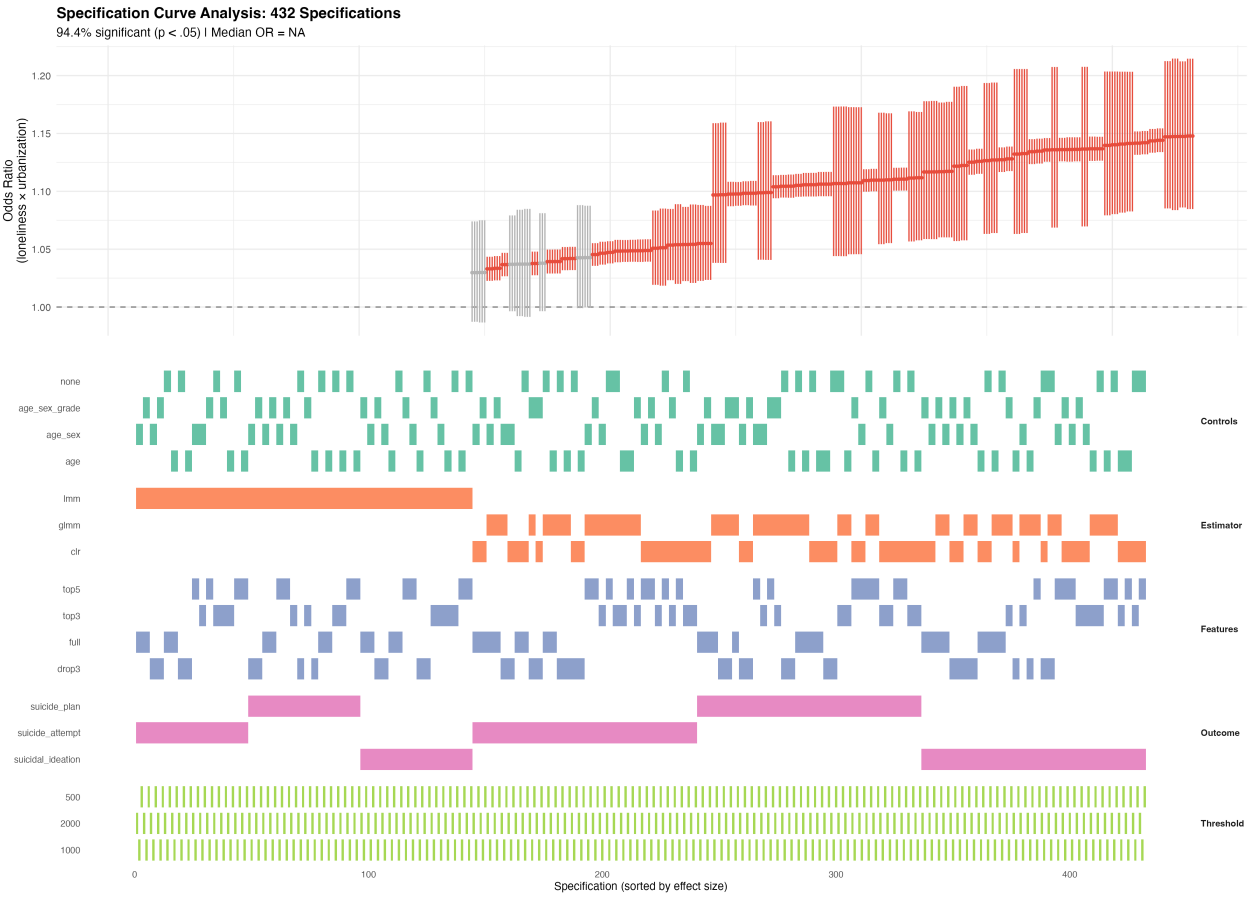


Figure 10: Specification Curve Analysis

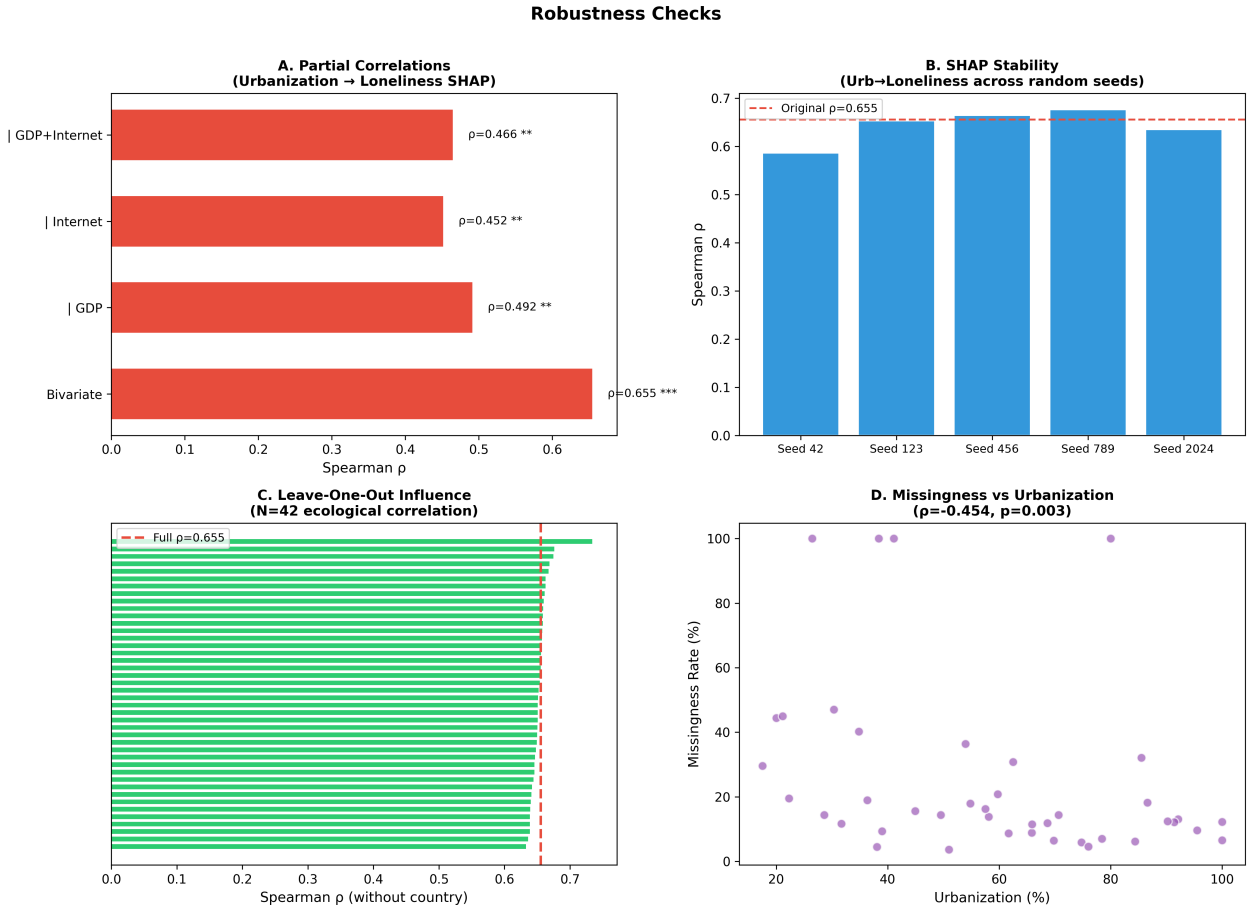


Figure 11: Robustness Checks

**Figure S12. Network Rewiring by Urbanization**
**Red edges (n = 5): strengthened in high-urbanization countries | Blue edges (n = 12): weakened | Gray edges (n = 88): non-significant**

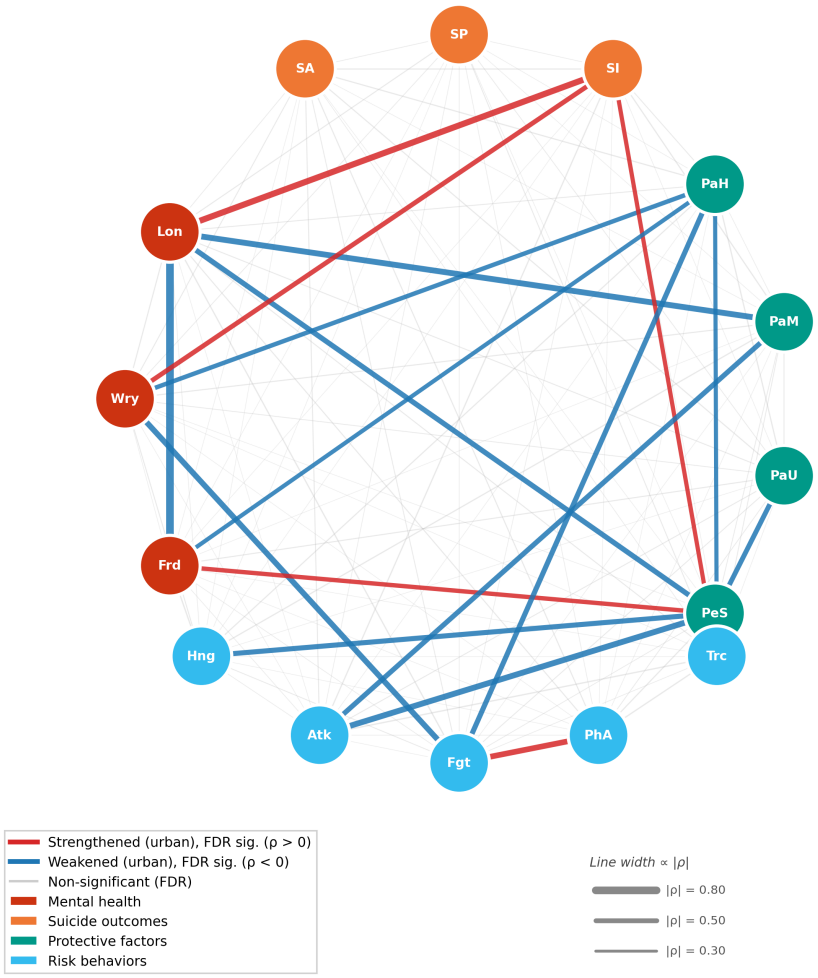


Figure 12: Network Rewiring by Urbanization

## Supplemental Analyses

### Supplemental Analysis 1: Stage 4 Sample Size Robustness Check

To assess whether country-level sample size (*N*) confounded the edge–urbanization associations, we examined the Spearman correlation between urbanization rate and sample size across the 38 countries included in Stage 4 (range: $N = 504–73{,}228$). The correlation was non-significant ($\rho = .299$, $p = .068$), indicating that more urbanized nations did not systematically contribute larger samples. As an additional robustness check, we recomputed Spearman partial correlations between each FDR-significant edge weight and urbanization, controlling for log-transformed sample size. All 17 FDR-significant edges remained significant after this correction (all $p\_FDR < .010$), with rank-correlation magnitudes largely unchanged (mean $|\Delta\rho| = .028$, range = .002–.113), and all direction signs were preserved. These results indicate that the observed edge–urbanization associations reflect genuine structural variation in psychological networks across countries, rather than an artifact of differential statistical power.

---

### Supplemental Analysis 2: Gender Gap and Urbanization

*Method.* Gender-stratified SHAP importance vectors were computed separately for males and females across 42 countries. Urbanization–loneliness SHAP correlations were compared between genders using a Fisher *z* test. The gender gap in suicidal ideation prevalence (female rate minus male rate) was correlated with urbanization rate.

*Results.* The loneliness × urbanization association was significant for females ($r\_s = .460$, $p = .002$) but non-significant for males ($r\_s = .202$, $p = .199$). A Fisher *z* test of gender differences did not reach significance ($p = .197$), and after FDR correction, none of the 12 features showed significant gender differences. The gender gap in suicidal ideation was positively correlated with urbanization rate ($r\_s = .495$, $p = .0009$): countries with higher urbanization had a larger female excess in suicidal ideation risk. This pattern is consistent with arguments regarding the disproportionate impact of social media on adolescent girls' mental health, though the non-significant Fisher *z* test means the gender difference in the urbanization–loneliness association itself was not statistically confirmed.

---

### Supplemental Analysis 3: Ising Computational Illustration

This post hoc computational illustration was not part of the original analytic pipeline. An Ising model was fitted to the global EBICglasso network, and comparative statics analysis was conducted via exact enumeration of the 2^14 = 16,384 state space (close friends was excluded due to a degenerate threshold parameter). Threshold parameters of four FDR-significant nodes (loneliness increased, worry-insomnia increased, hunger decreased, physical activity decreased) were modulated by urbanization level, simulating NIRA single-node deactivation intervention effects at different urbanization levels. Results showed that the loneliness intervention's effect on reducing suicidal ideation increased significantly with urbanization level (low urbanization

approximately 24% vs. high urbanization approximately 45%, Kruskal-Wallis $p < .001$), with a sigmoid inflection point at approximately 40% urbanization rate. This analysis represents comparative statics on cross-sectional parameters, not temporal prediction or causal claims, and is intended to translate Stage 3's statistical findings into an intuitively understandable network dynamics illustration (see Figure S9).

*Note on internal consistency check (not independent validation).* The Ising model parameters were derived from the same EBICglasso network used throughout the paper. A check of global NIRA output against empirical marginals yielded $\rho = 0.943$ (N = 14 nodes), and country-level comparison yielded $\rho = 0.658$ (N = 42 countries). In higher-urbanization countries, simulated lonely → SI activation was 45.2% vs. empirical 37.1%. These comparisons reflect internal consistency of the Ising parameterization, not external validation.

*Note on Specification Curve Analysis permutation test.* The 432 SCA specifications are not statistically independent, so the 94.4% significance rate is a descriptive consistency indicator rather than a formal inferential statistic. The permutation-based *p*-curve test recommended by Simonsohn et al. was computationally prohibitive for 432 multilevel models and was not conducted. SCA results therefore serve as sensitivity analysis rather than confirmatory inference.

---

*End of Supplementary Materials*